

TrkC plays an essential role in breast tumor growth and metastasis

Wook Jin*, Gyoung Mi Kim, Min Soo Kim, Mi Hee Lim, Chohee Yun¹, Joon Jeong², Jeong-Seok Nam³ and Seong-Jin Kim^{1,4}

Laboratory of Molecular disease and cell regulation, Lee Gil Ya Cancer and Diabetes Institute, Gachon University of Medicine and Science, Incheon 406-840, Korea, ¹Pediatric Oncology, Case Western Reserve University, Cleveland, OH 44106-7285, USA, ²Department of Surgery, Yong dong Severance Hospital, Yonsei University, Kangnam, Seoul 146-92, Korea and ³Laboratory of Tumor Suppressor, Lee Gil Ya Cancer and Diabetes Research Institute, Gachon University of Medicine and Science, Incheon 406-840, Korea and ⁴Laboratory of Cell Regulation and Carcinogenesis, Lee Gil Ya Cancer and Diabetes Institute, Gachon University of Medicine and Science, Incheon 406-840, South Korea

*To whom correspondence should be addressed.

Tel: +82 32 899 6417; Fax: +82 32 899 6039;

Email: jinwo@gachon.ac.kr

Correspondence may also be addressed to Wook Jin.

Tel: +82 2 3468 2646; Fax: +82 2 3468 2650;

Email: kimsj@cha.ac.kr

Tropomyosin-related kinase (Trk) C, a member of the Trk family of neurotrophin receptors, has been implicated in the growth and survival of human cancer tissues. Here, we report that TrkC is frequently overexpressed in human breast cancers and plays an essential role in tumor growth and metastasis. Ectopic expression of TrkC in non-malignant mammary epithelial cells suppressed anoikis, which correlated with activation of the Ras-mitogen-activated protein kinase and phosphatidylinositol-3-OH kinase (PI3K)/Akt pathways, and reduced expression of the metastatic regulator Twist. Furthermore, suppression of TrkC expression in highly metastatic mammary carcinoma cells inhibited their growth *in vitro*, as well as their ability to metastasize from the mammary gland to the lung *in vivo*. These results have identified TrkC as a critical regulator of breast cancer cell growth and metastasis.

Introduction

The tropomyosin-related kinase (Trk) family of neurotrophin receptors, TrkA, TrkB and TrkC, and their neurotrophin ligands primarily regulate growth, differentiation and survival of neurons (1,2). Neurotrophins and their corresponding receptors have been shown to induce a variety of pleiotropic responses in malignant cells, including enhanced tumor cell invasiveness and chemotaxis (3–7). TrkA and TrkB have been shown to be integrally involved in neuroblastoma biology (8,9), whereas TrkC is highly expressed in good-prognosis neuroblastomas as well as medulloblastomas (10–12). In studies of non-cutaneous cancers with a perineural invasive phenotype, such as prostate carcinoma, it has been shown that the tumor cells acquire an independent autocrine neurotrophin axis (13,14), and the observed perineural invasion is associated with high nerve growth factor/Trk presence (15). Roles for TrkA, TrkB and TrkC in carcinogenesis have also been shown in basal cell carcinoma and cutaneous squamous cell carcinoma (16). Malignant keratinocytes can express TrkA, B and C as a unique survival pathway, and elevated levels of expression of TrkA, B and C may predict perineural invasion in cutaneous squamous cell carcinoma. A recent study shows that TrkB is a potent and

Abbreviations: DMEM, Dulbecco's modified Eagle's medium; FBS, fetal bovine serum; MAPK, mitogen-activated protein kinase; MEK, MAP Kinase kinase; MFP, mammary fat pad; mRNA, messenger RNA; PARP, Poly (ADP-ribose) polymerase; PI3K, phosphatidylinositol-3-OH kinase; RT-PCR, reverse transcription-polymerase chain reaction; siRNA, Synthetic RNA interference; Trk, tropomyosin-related kinase.

specific suppressor of caspase-mediated anoikis in non-malignant epithelial cells (16). In this study, TrkB overexpression is shown to be sufficient to transform non-malignant cells into invasive and metastatic cells, by a mechanism that involves activation of the phosphatidylinositol-3-OH kinase (PI3K)/Akt pathway. This finding suggests that TrkB might drive one or more facets of tumor formation and metastasis.

Although classical activation of TrkC occurs by receptor multimerization in response to ligand binding, TrkC activation in human tumors seems to be largely attributable to overexpression of the full-length protein. A variety of non-neuronal tissues have been shown to express TrkC (4,10,16–19). A recent study shows that *trkC* gene in breast, lung and pancreatic cancers compared with normal tissues mutated within its kinase-encoding domain (20,21). The effect of these mutations on kinase function remains to be determined, but their positions within the protein suggest that many of them may affect kinase function. The growing evidence suggests that TrkC overexpression could contribute to tumorigenesis, invasion and the metastatic capability of cancer cells. Therefore, we examined the ability of TrkC to drive malignant pathophysiology in a mouse mammary tumor model and in human breast cancers.

Materials and methods

Cell culture and reagents

The breast cancer cell lines 67NR, 4T07, 4T1, ZR75B, SKBR3, MDA-MB-231 and Hs578T were purchased from American Type Culture Collection and maintained in Dulbecco's modified Eagle's medium (DMEM) high glucose (Gibco, Grand Island, NY) supplemented with 10% heat-inactivated fetal bovine serum (FBS), and the MCF7 cell line was maintained in RPMI1640 medium (Gibco) supplemented with 10% heat-inactivated FBS at 37°C in a humidified 5% CO₂ incubator. Antibodies were obtained from the following companies: anti-TrkC (C-14, 798), anti-HA(Y-11), anti-cyclin D1 (M-20) and anti-Myc (9E10), from Santa Cruz Biotechnology (Santa Cruz, CA); anti-V5 from Invitrogen (Carlsbad, CA); anti-phospho-MAP kinase kinase (MEK)1/2, anti-p44/42 mitogen-activated protein kinase (MAPK), anti-Poly (ADP-ribose) polymerase (PARP), anti-caspase-3 and anti-phospho-Akt from Cell Signaling Technology (Danvers, MA) and anti-β-actin from Sigma-Aldrich (St. Louis, MO). The protein kinase inhibitors K252a, LY294002 and U0126 were purchased from Calbiochem (Gibbstown, NJ).

Plasmids

Each of the two Synthetic RNA interference (siRNA)-encoding oligonucleotides against mouse TrkC were designed and verified to be specific to TrkC by BLAST search against the mouse and human genomes, respectively. To construct hairpin-type single RNA interference vectors, 5 μl (100 mM) of the synthesized sense and antisense oligonucleotides (supplementary Table 1 is available at *Carcinogenesis* Online) were combined with 1 μl of 1 M NaCl and annealed by incubation at 95°C for 2 min, followed by rapid cooling to 72°C and ramp cooling to 4°C over a period of 2 h. The mouse TrkC-siRNA insert was subcloned into the XbaI/XhoI site of pFG12 lentiviral vector. A Control-siRNA, which does not match any known mouse coding complementary DNA, was used as a control.

Human tumor samples

Protein and RNA of human tissue samples were obtained from the Gangnam Severance Hospital after approval by the institutional review board and ethics committee of Gangnam Severance Hospital.

Immunoblotting and immunoprecipitation

Cells were lysed in a buffer containing 25 mM *N*-2-hydroxyethylpiperazine-*N'*-2-ethanesulfonic acid (pH 7.5), 150 mM NaCl, 1% Triton X-100, 10% glycerol, 5 mM ethylenediaminetetraacetic acid and protease inhibitor mixture (Complete; Roche, Gifp-Oberfrick, Switzerland). Extracts were separated by sodium dodecyl sulfate/polyacrylamide gel electrophoresis followed by electrotransfer to poly(vinylidene difluoride) membranes and probed with polyclonal or monoclonal antisera, followed by horseradish peroxidase-conjugated secondary antibodies and visualized by chemiluminescence according to the manufacturer's instructions (Pierce, Rockford, IL). For immunoprecipitation, the cell lysates were incubated with the appropriate antibody for 1 h, followed

by incubation with Gamma-bind beads GE Healthcare Co. (Piscataway, NJ) for 1 h at 4°C. Beads were washed four times with the buffer used for cell solubilization. Immune complexes then were eluted by boiling for 3 min in 2× Laemmli buffer (pH 6.8) and then extracts were analyzed by immunoblotting as described above.

Soft agar assays

Soft agar assays were performed according to established protocols. 67NR and 4T1 cells infected with recombinant lentiviruses carrying either an empty vector or an TrkC-siRNA were seeded in triplicate at a density of 8×10^3 cells per well in a six-well plate. Bottom layers were made up of 0.4% agar in 9% FBS and DMEM. Cells were resuspended in a top layer of 0.2% agar in 9% FBS and DMEM. Cells were fed every other day by placing two drops of medium on the top layer. After 3 weeks at 37°C, colonies were stained with *p*-iodonitrotetrazolium violet (2 µg/ml) for 16 h and macroscopic colonies were counted (in quadruplicate).

Matrigel invasion assay

Breast cancer cell invasion was assayed in 24-well Biocoat Matrigel invasion chambers (8 µm; BD Biosciences, Bedford, MA) according to the manufacturer's protocol. Briefly, the top chamber was seeded with 2.5×10^5 viable tumor cells in a serum-free medium with 0.5% bovine serum albumin. The bottom chamber was filled with DMEM supplemented with 10% FBS as a chemoattractant. After 16 h of incubation, the non-invasive cells that remained on the upper surface of the membrane were removed with a cotton swab. Cells that had invaded through the membrane were then fixed with methanol and stained with hematoxylin (Vector, Burlingame, CA). Invasive cells per field were counted for three random fields for each membrane, using a light microscope at ×200 magnification. Invasion assays were performed in triplicate.

Anchorage-independent cell growth

67NR and 4T1 cells infected with recombinant lentiviruses carrying either an empty vector or an TrkC-siRNA were seeded into an Ultra Low Cluster plate (Corning Life Sciences, Acton, MA) at 1×10^6 cells and photographed at 96 h.

Viral production and infection of target cells

293T cells were transfected with the transfer vector plasmid pFG12-siLuc (empty) or pFG12-Mouse siTrkC (1604, 216) plasmid with the envelope-encoding plasmid pHCMVG, the packaging plasmid pMDLg/pRRE and the Rev-expression plasmid pRSV-Rev using the calcium phosphate method. The supernatants were harvested 48 and 72 h after transfection, pooled, passed through a 0.45 µm filter, ultracentrifuged for 2 h at 100 000g, resuspended in 100 µl of 0.1% bovine serum albumin in phosphate-buffered saline, and the lentivirus stocks were stored in small aliquots at −80°C for titration and cell infection. 67NR, 4T1 and Hs578T cells were plated in six-well plates (1×10^5 cells per well) and were cultured overnight. Lentiviruses were diluted in 2 ml DMEM containing polybrene (8 µg/ml) and then centrifuged for 30 min at 1500 r.p.m. Twenty-four hours after infection, polybrene-DMEM was replaced with fresh DMEM medium and the cells were cultured for other assays.

In vivo tumorigenicity and metastasis assay

All animals were maintained according to the National Cancer Institute's Animal Care and Use Committee guidelines, under approved animal study protocols. For the spontaneous metastasis format, the left inguinal (#4) mammary glands of anesthetized 7-week-old female BALB/cANCr mice (National Cancer Institute-Frederick, Frederick, MD) were surgically exposed and 2×10^5 4T1 cells (wild-type, Control-siRNA-expressing or si-TrkC-expressing) were inoculated into the mammary fat pad (MFP) in a volume of 40 µl. The mice ($n = 5-10$ for each group) were euthanized 28 days after inoculation. At the sacrifice time point, the MFP primary tumor and lungs were removed and fixed in 10% buffered formalin. The MFP tumor volume was calculated by the formula ($S \times S \times L$) × 0.52, where *S* and *L* were the short and long dimensions, respectively. Macroscopic quantitation of metastases was performed by counting the number of nodules on the surface of the lung. For microscopic quantitation of lung metastases, each lobe of the lung was processed for hematoxylin and eosin staining and evaluated by independently by two observers (W.J. and C.Y.).

Reverse transcription-polymerase chain reaction

Total RNA was extracted using a Quizol reagent (Qiagen, Inc., Valencia, CA). Reverse transcription was done using a one step Reverse transcription-polymerase chain reaction (RT-PCR) kit according to the manufacturer's instructions (Qiagen, Inc.). Mouse *TrkC* RT-PCR forward primer is 3'-CTTAAACAAGTTCCTCAGGGCCCAT-5' and its RT-PCR reverse primer is 3'-AAGAATGTCCAGGTAGATCGGGGT-5'. Mouse *Twist-1* RT-PCR forward primer is 3'-CGGGTCATGGCTAACGTG-5' and its RT-PCR reverse primer is 3'-CAGCTTGCCATCTTGAGATC-5'. Human *TrkC* RT-PCR for-

ward primer is 3'-CTCTCCCAAATGCTCCACAT-5' and its RT-PCR reverse primer is 3'-TCCGGTACA TGATGCTTTCA-5'. Mouse and human *Gapdh* (Glyceraldehyde 3-phosphate dehydrogenase) RT-PCR forward primer is 3'-GACCCCTTCATTGACCTCAAC-5' and its RT-PCR reverse primer is 3'-CTTCTCCATGGTGGTGAAGA-5'. Polymerase chain reaction products were separated on 1% agarose gels and visualized by ethidium bromide.

Immunohistochemistry

Routine formalin-fixed and paraffin-embedded excision biopsies of a series of primary tumor and lung formed by 4T1 cells expressing either control-siRNA or TrkC-siRNAs were analyzed. Immunohistochemistry was performed on 5 mm tissue sections. All specimens were immunostained with a non-biotin detection system (Bond Polymer Refine; Leica Microsystems, Bannockburn, IL), with diaminobenzidine development. Heat-induced antigen retrieval was performed using Tris-ethylenediaminetetraacetic acid buffer (pH 9.0) in a water bath at 95°C for 30 min. Monoclonal anti-TrkC (clone 4G5, Abcam, Cambridge, MA) were used. Stainings were performed with an automatic immunostainer (Bond System; Leica Microsystems, Bannockburn, IL).

Cell viability assay

The cell viability assay was performed using 3-(4,5-dimethylthiazole-2-yl)-2,5-diphenyl tetrazolium bromide assay, which determines mitochondrial activity in living cells. The cells were plated in 96-multiwell plates at a density of 1×10^4 cells per well and 100 µl of DMEM containing 3-(4,5-dimethylthiazole-2-yl)-2,5-diphenyl tetrazolium bromide (0.5 mg/ml) was added to each well and incubated in CO₂ at 37°C for 3 h. After the incubation period, the media were removed and the cells were washed twice with phosphate-buffered saline. The living cells can transform the tetrazolium ring into dark blue insoluble formazan crystals solubilized with dimethyl sulfoxide, which can be quantified at 570 nm using an enzyme-linked immunosorbent assay reader.

Analysis of apoptosis by annexin staining

4T1 cells expressing control-siRNA or TrkC-siRNAs and 4T1 cell treated with K252a, LY294002 and U0126 were each seeded at a density of 1×10^6 cells/ml in 60 mm culture dishes and incubated for 24 h in a CO₂ incubator. Apoptosis was determined by an Annexin-V apoptosis detection kit (BD Pharmingen™, San Jose, CA) according to the manufacturer's protocol. Flow cytometric data of 10 000 cells per sample were acquired on a FACS Calibur (Franklin Lakes, NJ). Data were analyzed using the computer program Win MDI 2.8.

Results

Expression of TrkC in human breast tumor samples

TrkC is reported to be overexpressed in breast cancers compared with normal tissues (22) and in brain metastases of breast carcinomas (23). However, relatively little is known about whether TrkC activation is essential for its contribution to the malignant properties of human tumors. To further evaluate whether TrkC is an essential contributor to carcinoma progression, we first determined whether expression of TrkC correlated with certain pathological phenotypes in clinical breast tumor samples. To do so, we measured TrkC messenger RNA (mRNA) and protein expression in 38 normal and invasive human breast tumors and compared these findings with histopathological criteria. About 84% of infiltrating ductal carcinoma (32 of 38 tumor samples) showed elevated TrkC expression compared with normal their normal counterparts (Figure 1A and supplementary Figure 1A and B is available at *Carcinogenesis* Online). We next examined the elevated levels of TrkC associated with the increase in phosphorylation of TrkC. Total tissue extracts were subjected to immunoprecipitation with the anti-TrkC antibody followed by immunoblotting with the anti-phospho-tyrosine antibody. As shown in Figure 1A, TrkC phosphorylation strongly increased in invasive human breast tumors, suggesting that expression of TrkC may contribute to the pathogenesis of human invasive breast carcinomas. We next examined TrkC expression in a mouse mammary model system that consists of three distinct tumor cell lines: 67NR, 4TO7 and 4T1. All three cell lines are derived from a single mammary tumor that arose spontaneously in a wild-type BALB/c mouse. 67NR cells form primary tumors but cannot disseminate to distant tissues, including blood, lymph nodes and lung. 4TO7 cells are able to spread from the primary site to the lung but cannot establish visible metastatic nodules. 4T1 cells are the most aggressive, able to complete all steps of metastasis and efficiently form visible metastatic nodules in the

lung (24). Together, these tumor lines reflect the sequence of multistep metastatic progression and therefore represent a valuable tool for examining the role of Trk proteins in mammary tumorigenesis and metastasis. We first compared the expression of neurotrophin receptors in these cells and found that all three cell lines had low to undetectable *trkA* and *trkB* expression; RT-PCR analysis showed that the 67NR cell line had negligible *trkC* expression, whereas *trkC* mRNA was expressed in 4T07 and 4T1 cell lines, with 5- to 10-fold higher levels detected in 4T1 tumor cells compared with 4T07 cells

(Figure 1B). Correspondingly, we also observed expression of TrkC protein in 4T07 and 4T1 tumor cells but not in 67NR cells and analysis of tyrosine phosphorylation indicated that TrkC was tyrosine phosphorylated in 4T07 and 4T1 cells, indicating an activated state (Figure 1B).

To determine whether TrkC is an important mediator of the tumorigenic capacities of the highly aggressive 4T1 cells, we examined whether pharmacological inhibition of TrkC with CEP-701, an inhibitor of the Trk (NTRK) tyrosine kinases, would influence the ability of

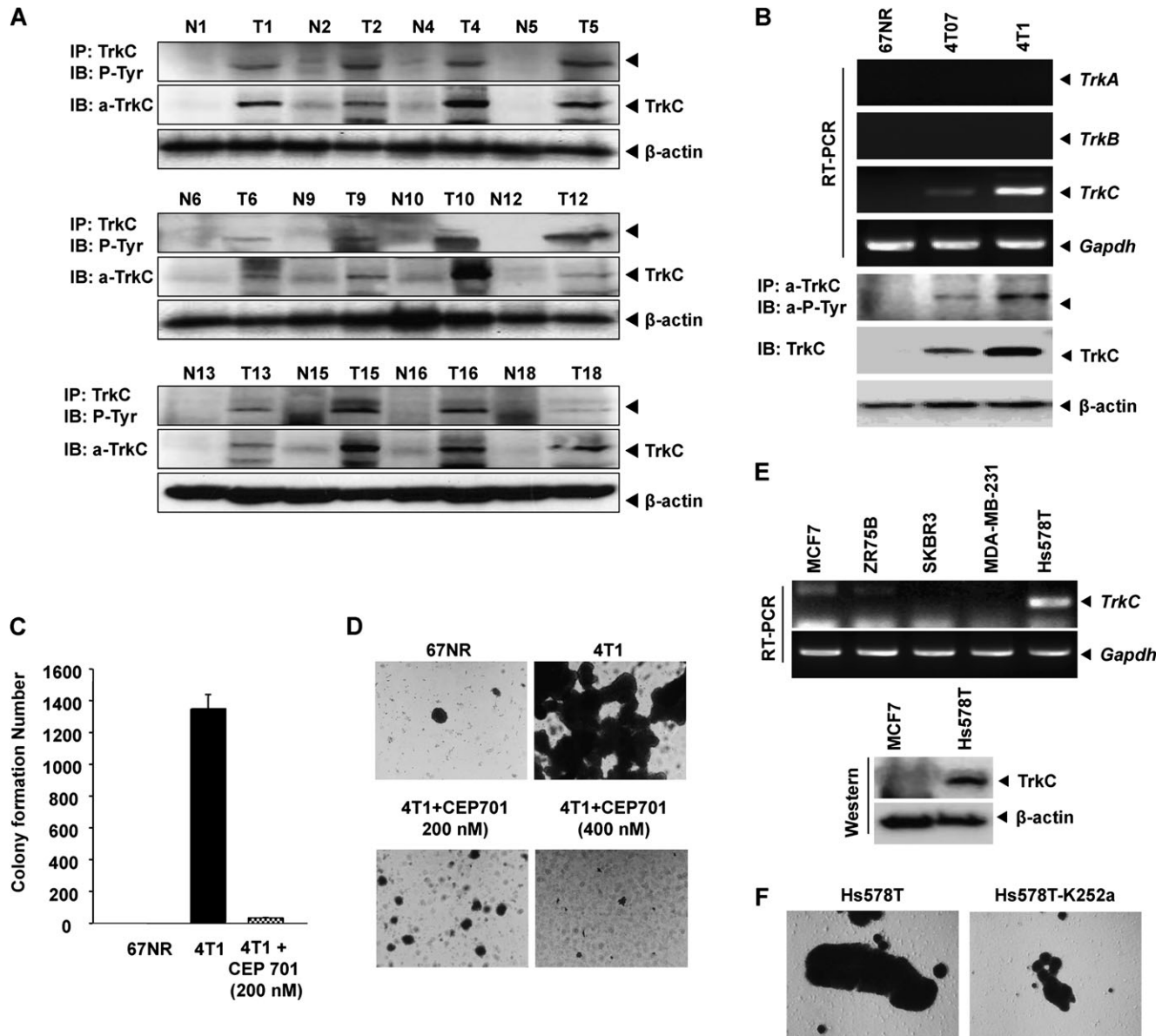


Fig. 1. TrkC is overexpressed in mouse and human breast cancer cell lines and the inhibition of TrkC blocks colony formation and anchorage-independent growth of 4T1 cells. (A) The expression profile of TrkC in human primary tumors. The RNA and protein of primary breast tumor tissue and normal tissue from breast cancer patients were subjected to immunoprecipitation using anti-TrkC antibody, followed by immunoblotting with anti-TrkC antibody or anti-phospho-tyrosine antibody. The endogenous β -actin levels were measured as internal controls. (B) Relative expression of TrkA, TrkB and TrkC in mouse breast cell lines (67NR, 4T07 and 4T1) was examined by RT-PCR. The endogenous *Gapdh* mRNA levels were measured as internal controls. Assessment of TrkC phosphorylation in mouse breast cancer cell lines (67NR, 4T07 and 4T1). Cell extracts were immunoprecipitated using anti-TrkC antibody and Gamma-bind beads (Amersham Pharmacia Biosciences), followed by immunoblotting with anti-phospho-tyrosine antibody (lower panel). (C) Soft agar colony-forming assay of mouse breast cancer cell lines. Monolayer cells were trypsinized, washed and plated in medium containing 0.2% agar to assess anchorage-independent growth. Results are presented as the number of macroscopic colonies formed at 3 weeks after plating. (D) The 4T1 and 67NR mouse breast cancer cell lines seeded in presence of serum into ultralow cluster plates and treated with CEP701 (200 nM) or vehicle control (dimethyl sulfoxide) for 7 days. Spheroid formation then photographed at $\times 200$ magnification. (E) Expression of TrkC in human breast cell lines was examined by RT-PCR and immunoblotting. Endogenous *Gapdh* mRNA levels and β -actin levels were measured as internal controls. (F) Hs578T cells treated after spheroid formation with K252a (200 nM), photographed at $\times 50$ magnification 3 days later.

4T1 cells to survive and proliferate in an anchorage-independent manner. Pretreatment with CEP-701 has been shown to completely abolish neurotrophin-3 (NT-3)-induced tyrosine phosphorylation of NTRK3 (25). After growing in soft agar for 15 days, 4T1 cells grown in the presence of CEP-701 formed significantly fewer colonies than untreated cells (Figure 1C). This result suggested that TrkC could be affecting the survival of 4T1 cells. It is known that normal epithelial cells undergo programmed cell death in response to deprivation of their extracellular matrix, by a process called anoikis. To mimic anoikis *in vitro*, we used cell culture dishes to which 4T1 cells could not attach. Under these conditions, 4T1 cells proliferated as large spheroid aggregates in suspension, whereas treatment of 4T1 cells with CEP-701 markedly suppressed survival of 4T1 cells in suspension (Figure 1D). This result suggested that TrkC promotes the survival of 4T1 cells, perhaps by suppressing anoikis. To further investigate the functional role of TrkC in apoptosis, we examined a cell viability assay using 4T1 cells treated with K252a and 4T1 cells expressing either control-siRNA or TrkC-siRNA. Growth of 4T1 cells treated with K252a and 4T1 cells expressing TrkC-siRNA were significantly inhibited compared with the control cells (supplementary Figure 2A and E is available at *Carcinogenesis* Online). We examined whether pharmacological inhibition of TrkC with K252a, an inhibitor of the Trk (NTRK) tyrosine kinases, would influence the ability of 4T1 cells to survive and proliferate. Indeed, 4T1 cells treated with K252a grew more slowly than the parental cells (supplementary Figure 2D is available at *Carcinogenesis* Online). Next, to identify the inhibition mechanism of apoptosis by TrkC, we investigated the activation of caspase-3 and the cleavage of PARP. As shown in supplementary Figure 2B and F (available at *Carcinogenesis* Online), the 4T1 cells expressing TrkC-siRNA and 4T1 cells treated with K252a significantly increased the activation of caspase-3 and the cleavage of PARP (an endogenous substrate of caspase-3) in comparison with the control. To further characterize inhibition of apoptosis by TrkC, we assessed the translocation of phosphatidylserine using annexin V. As shown in supplementary Figure 2C and G (available at *Carcinogenesis* Online), cell numbers in lower right quadrants, which correspond to early apoptosis cells (annexin V-positive), were increased up to 17-fold in 4T1 cells expressing TrkC-siRNA and 4T1 treated with K252a but 4T1 cells markedly decreased. To determine whether TrkC might play a role in inducing the tumorigenic or metastatic properties of human breast cancers, we examined whether TrkC expression was detectable in several invasive human breast tumor cell lines, such as MCF7, ZR-75, SKBR3, Hs578T and MDA-MB-231. We only observed TrkC expression at the mRNA and protein level in the Hs578T cell line, one of the invasive and metastatic human tumor cell lines. In contrast, non-metastatic tumor cell lines, such as MCF7, ZR-75 and SKBR3, did not express TrkC (Figure 1E). We also examined whether TrkC functioned to suppress anoikis in these cells, as was observed in the 4T1 model; indeed, whereas untreated Hs578T cells proliferated as large spheroid aggregates in suspension, treatment of Hs578T cells with K252a markedly suppressed survival of Hs578T cells in suspension (Figure 1F).

TrkC is essential for tumor growth and can promote invasion

To further investigate the functional role of TrkC in breast cancer progression, we used siRNA technology to knockdown TrkC expression in the highly metastatic 4T1 cells. This was achieved by designing siRNA molecules that target sequences in the coding region of the mouse *trkC* gene, infecting 4T1 cells with lentivirus encoding these siRNAs and then selecting the cells stably expressing the siRNAs and assessing knockdown efficiency. As shown in Figure 2A, expression of two different siRNAs each markedly reduced the expression of *trkC* mRNA and TrkC protein in 4T1 cells. A luciferase siRNA, whose sequence did not match any known mouse gene, was used as a control.

As mentioned previously, the *trkC* gene is also known to be a partner in the formation of the *ETV6-NTRK3 (Tel-TrkC)* fusion gene. *ETV6-NTRK3* appears to be linked to both the Ras-Erk1/2 and the PI3K-Akt pathways (26,27). We next examined the activation of the Ras-MAPK and PI3K-Akt pathways, as well as cyclin D1

expression, in pools of 4T1 cells in which TrkC expression was silenced. Although levels of phosphorylated (activated) MEK1/2 and PI3K-Akt, as well as cyclin D1 expression, were markedly higher in 4T1 cells compared with 67NR cells, knockdown of TrkC in the 4T1 cells significantly reduced levels of phosphorylated MEK1/2 and Akt as well as cyclin D1 expression (Figure 2B). Akt is a serine/threonine kinase belonging to the cyclic adenosine 3',5'-monophosphate-dependent protein kinase A/protein kinase G/protein kinase C superfamily of kinases. Its activation is induced in the course of signal transduction by growth factors or insulin and it is involved in many cellular processes, such as cell growth and survival, glucose metabolism and transcriptional regulation (28). Akt is activated by phosphorylation at both serine 308 and serine 473 by a kinase pathway initiated by PI3K. The majority of the data indicate that Akt has critical roles in cell growth, survival and apoptosis blockage by promoting the phosphorylation and subsequent cytoplasmic localization of many downstream proapoptotic protein targets (29). Consistent with this, Akt signaling has been shown to be pretumorigenic. Immunohistochemistry studies have demonstrated that Akt is highly phosphorylated at serine 473 in the majority of primary invasive breast tumors (30). Since our data show that TrkC expression correlates with Akt activity, we examined whether the phosphorylation status of Akt in primary invasive breast tumor samples and adjacent normal tissue correlated with TrkC expression in the same samples. Indeed, Akt was found to be highly phosphorylated in primary invasive breast tumor samples, which express TrkC protein (Figure 2C). To further investigate whether the activation of Akt and MAPK by TrkC inhibits apoptosis, we examined whether pharmacological inhibition of Akt or MEK1/2 with either LY294002, an inhibitor of PI3K or U0126, an inhibitor of MEK1/2 would influence the ability of 4T1 cells to survive and proliferate. Indeed, 4T1 cells treated with either LY294002 or U0126 grew more slowly than parental cells (supplementary Figure 3A is available at *Carcinogenesis* Online). We examined cell viability assay using 4T1 cells treated with either LY294002 or U0126. Growth of 4T1 cells treated with either LY294002 or U0126 significantly inhibited compared with the control cells (supplementary Figure 3B is available at *Carcinogenesis* Online). Next, we investigated the activation of caspase-3 and the cleavage of PARP. As shown in supplementary Figure 3C (available at *Carcinogenesis* Online), the 4T1 cells treated with either LY294002 or U0126 significantly increased the activation of caspase-3 and the cleavage of PARP (an endogenous substrate of caspase-3) in compared with control. To further characterize inhibition of apoptosis by Akt and MEK1/2 activation in 4T1, we assessed the translocation of phosphatidylserine using annexin V. As shown in supplementary Figure 3D (available at *Carcinogenesis* Online), cell numbers in lower right quadrants, which correspond to early apoptosis cells (annexin V-positive), were significantly increased in 4T1 cells treated with either LY294002 or U0126 but 4T1 cells markedly decreased. This result suggested that activation of Akt and MEK1/2 by TrkC inhibits apoptosis. We next examined whether knockdown of TrkC expression affects the ability of 4T1 cells to proliferate and invade *in vitro*. Indeed, si-TrkC-expressing 4T1 cells grew more slowly than both parental cells and 4T1 cells expressing control-siRNA (Figure 2D). We also examined whether knockdown of TrkC affects anchorage-independent growth of 4T1 cells. After growing in soft agar for 15 days, 4T1 cells expressing *trkC*-siRNAs formed a significantly lower number of colonies (Figure 2E).

Knockdown of TrkC significantly reduces colony formation *in vitro* and tumor growth *in vivo*. To determine whether TrkC also plays an important role in cancer invasion and metastasis, invasion through Matrigel was assessed in 4T1 *trkC*-siRNA cells and the 4T1 control-siRNA cells. In *in vitro* invasion assays, the pooled 4T1 *trkC*-siRNA cells showed a 4- to 8-fold reduction in ability to invade through Matrigel compared with parent and control cells (Figure 2F). In addition to being a direct effect on invasiveness, we should note that the decreased invasion may also be due to a decreased proliferation rate as this was shown to be an additional consequence of TrkC inhibition (Figure 2E).

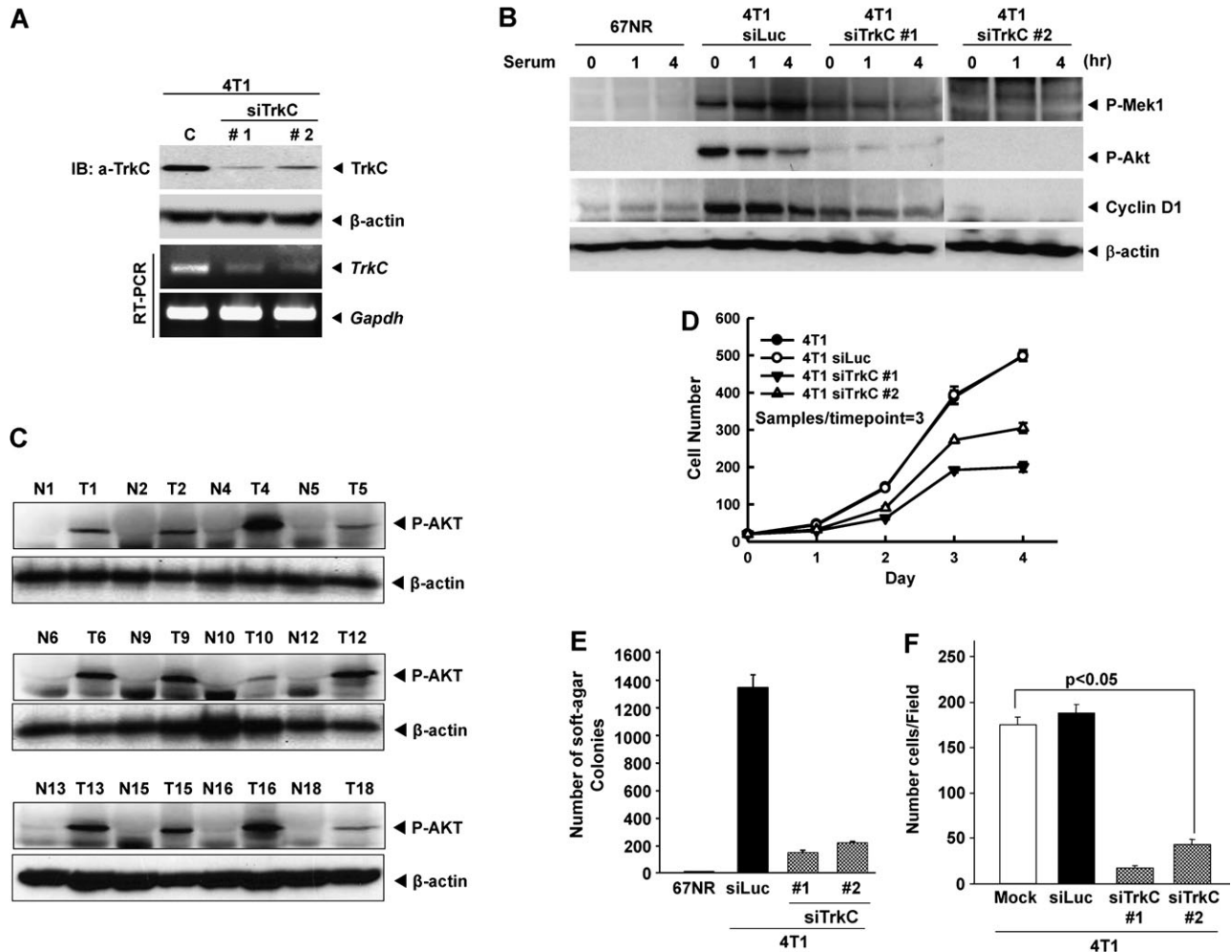


Fig. 2. Suppression of TrkC expression by stable TrkC-siRNA reduces cell proliferation and colony formation. (A) The protein and RNA of TrkC expression were examined by immunoblotting and RT-PCR in 4T1 cells stably expressing Control-siRNA, TrkC-siRNA #1 or TrkC-siRNA #2. The endogenous β -actin and *Gapdh* mRNA levels were measured as internal controls. (B) Parental 4T1 and 4T1 cells expressing either control-siRNA or TrkC-siRNAs were serum starved overnight in 0.5% serum and then stimulated with and without 10% FBS at the indicated times (0, 1, 4 and 6 h). Whole-cell lysates were prepared for western blotting and probed with antibodies against the phosphorylated forms of Mek1/2 (ser217/221), phosphorylated Akt (Ser 473) and cyclin D1. (C) The expression profile of phospho-Akt in human primary tumors. The protein of primary breast tumor tissue and normal tissue from breast cancer patients was subjected to immunoblotting with antiphospho-Akt antibody. The endogenous β -actin levels were measured as internal controls. (D) Population doublings of wild-type 4T1 and 4T1 cells expressing either control-siRNA or TrkC-siRNAs. Each data point represents the mean of cells counted in triplicate dishes. (E) Anchorage-independent growth of 67NR control cells or 67NR and 4T1 cells expressing either control-siRNA or TrkC-siRNAs. The number of soft agar colonies presented is the mean of colony counts in $\times 50$ microscopic fields from three dishes. (F) Cell invasion assay. Parental 4T1 and 4T1 cells expressing either control-siRNA or TrkC-siRNAs were induced to invade toward serum. After 16 h of incubation, cells that traversed the Matrigel-coated filters were stained and counted ($P < 0.05$).

To explore whether increased expression of TrkC could stimulate breast cancer progression-related biological responses, 67NR cells were infected with recombinant retroviruses carrying a *TrkC* complementary DNA or empty MSCV vector as a control. Individual positive transformants were obtained by puromycin selection. Expression of the predicted 140 kD TrkC protein in transformed cells was verified by immunoblotting using the anti-TrkC (C-14) antibody (Figure 3A). We also examined whether the ectopically expressed TrkC was phosphorylated in these cells; all TrkC in 67NR cells expressing TrkC appeared to be autophosphorylated, probably by endogenous NT-3 (Figure 3A). To test whether TrkC expression affects the Ras-Erk1/2 and the PI3K-Akt pathways, we examined the activation states of MEK1/2 and Akt as well as total cyclin D1 levels in 67NR cells expressing TrkC. Levels of phosphorylated MEK1/2 and Akt, as well as cyclin D1 expression, were enhanced markedly in TrkC-expressing cells (Figure 3B). We also examined whether TrkC expression affects the anchorage-independent growth of 67NR cells. After growing in soft agar for 15 days, 67NR cells expressing *trkC* formed colonies; this was not seen in control cells (Figure 3C). Together, these data

demonstrate that TrkC induces the activation of Ras-Erk1/2 and the PI3K-Akt pathways, events that may support the growth and tumorigenicity of breast tumors.

Twist is a highly conserved basic helix-loop-helix transcription factor, which is implicated as an oncogene. A recent study showed that Twist, a master regulator of morphogenesis, plays an essential role in metastasis and that *Twist* mRNA is expressed in 4T1 cells (31). To elucidate association between TrkC and Twist, we examined whether expression of TrkC was able to induce endogenous *Twist* gene in 67NR cells; indeed, the expression of *Twist* gene was markedly enhanced in 67NR cells overexpressing TrkC (Figure 3D). Therefore, we also examined whether knockdown of TrkC affects the expression of Twist in 4T1 cells. Indeed, knockdown of TrkC reduced expression of *Twist* gene (Figure 3E). To see whether the increasing levels of TrkC further activate Twist-1, we transfected TrkC in T-47D tet-on cell lines using a tetracycline-inducible system and examined the Twist activation. The expression of TrkC was conditionally regulated by the application of doxycycline and we demonstrated that the expression level of *Twist* genes was increased

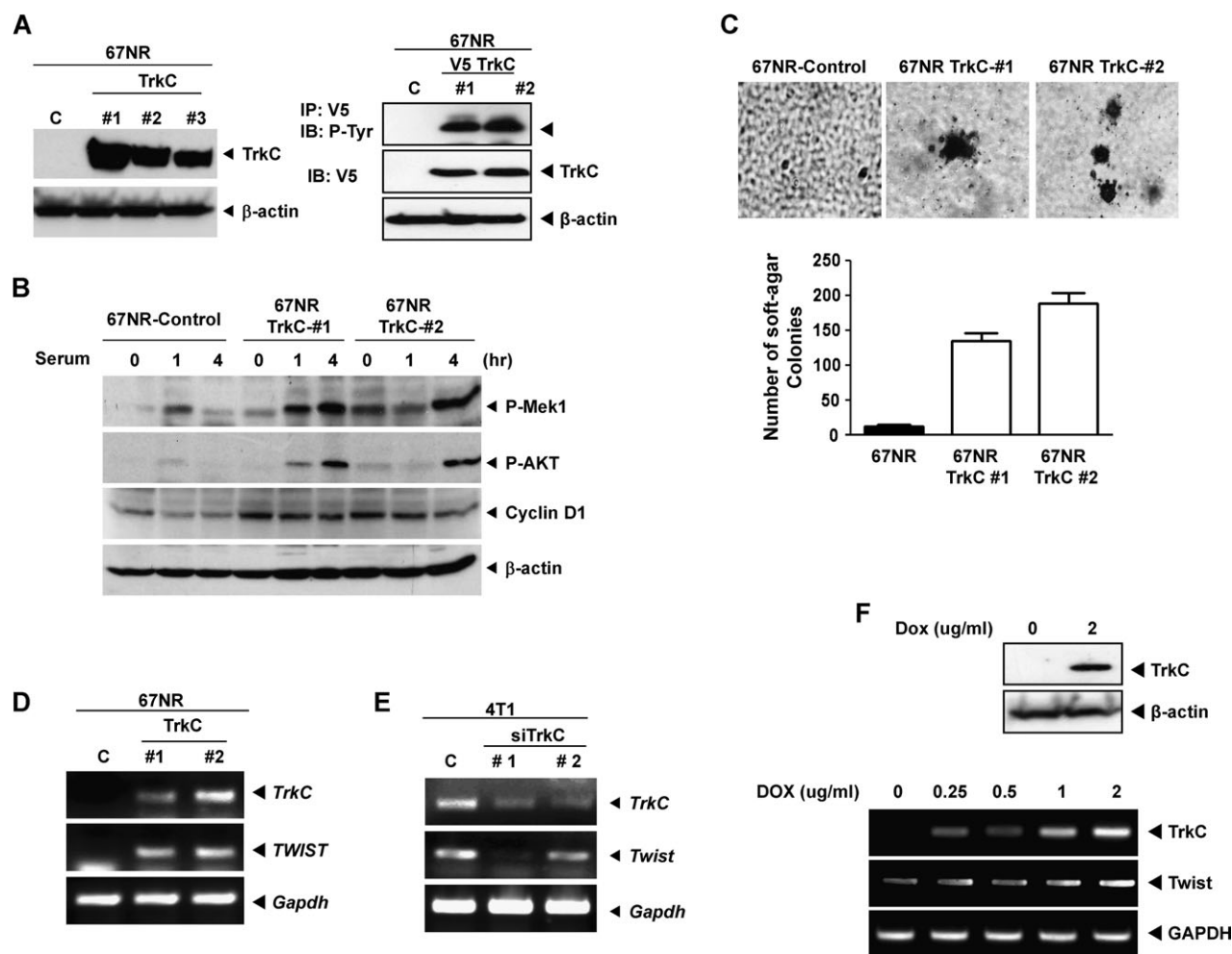


Fig. 3. TrkC induces elevated levels of phosphorylated Akt, phosphorylated MEK1, Twist-1 and cyclin D1. (A) Analysis of TrkC protein expression using anti-TrkC antibody (left panel). Assessment of TrkC phosphorylation in 67NR cell lines stably expressing control vector or TrkC. Cell extracts were immunoprecipitated using anti-V5 antibody and Gamma-bind beads (Amersham Pharmacia Biosciences), followed by immunoblotting with anti-phospho-tyrosine antibody (right panel). (B) Immunoblot analysis of the phosphorylated forms of Mek1/2 (ser217/221), phosphorylated Akt (Ser 473) and cyclin D1 in 67NR cells expressing a control vector or TrkC. (C) Anchorage-independent growth of 67NR control cells or 67NR and 4T1 cells expressing either control-siRNA or TrkC-siRNAs. The number of soft agar colonies presented is the mean of colony counts in $\times 50$ microscopic fields from three dishes. Representative photos are presented as macroscopic colonies formed at 3 weeks after plating. (D) RT-PCR analysis of *TrkC* and *Twist* mRNA expression in 67NR cell lines stably expressing control vector or TrkC. (E) Expression of *TrkC* and *Twist* mRNAs was examined by RT-PCR in 4T1 cells stably expressing Control-siRNA, TrkC-siRNA #1 or TrkC-siRNA #2. The endogenous *Gapdh* mRNA levels were measured as internal controls. (F) Induction of TrkC expression by doxycycline increased the level of Twist-1 in T-47D tet on cells. Cells were cultured for 0–48 h in the presence (2 μ g/ml) and absence of doxycycline. The protein and RNA of TrkC and Twist expression were examined by immunoblotting and RT-PCR.

depended on TrkC expression (Figure 3F). These results suggest that TrkC is a regulator of Twist expression and indicates that elevated TrkC expression might therefore contribute to the malignant behavior of breast tumors through the induction of these important oncogenic mediators.

Knockdown of TrkC significantly reduces tumor growth and metastasis *in vivo*

To determine whether TrkC plays a causal role in tumor growth and metastasis, we tested whether suppression of TrkC expression in the highly metastatic 4T1 cells would affect their growth potential and metastatic ability *in vivo*. We injected pools of 4T1 cells carrying either the *trkC*-siRNAs or the control-siRNA into the MPFs of BALB/c mice and measured the growth of the resulting primary tumors weekly. Parental and si-control 4T1 cells formed primary mammary tumors at identical rates, whereas primary tumor formation by 4T1 cells carrying either of the two *trkC*-siRNAs was markedly decreased (Figure 4A and B). Histological examination revealed that the primary tumors formed by the *trkC*-siRNA cells and the control-siRNA cells

were both undifferentiated mammary carcinomas (Figure 4C). We then performed immunohistochemistry with a TrkC-specific antibody on tumor tissues. Interestingly, TrkC expression reduced in primary tumors from mice injected with the *trkC*-siRNA-expressing cells when compared with the control counterparts and an enhanced expression of TrkC is seen in cancer cells with spindle shaped Sarcomatous morphology (Figure 4D). We believe that primary tumors formed by the injection of the *trkC*-siRNA cells may have arisen from 4T1 cells in which TrkC expression was minimally suppressed since we used pooled populations of *trkC*-siRNAs without clonal selection. As shown Figure 2A, knockdown of *trkC* was not complete in the 4T1 *trkC*-siRNA stable cell lines. Our results suggest that TrkC is required for primary tumor formation by 4T1 cells.

To determine whether loss of TrkC expression affects the ability of 4T1 cells to metastasize *in vivo*, we examined the metastatic capacity of 4T1 cells expressing either the *trkC*-siRNAs or the control-siRNA. Four weeks after mammary gland implantation of cells, mice were killed and the lungs were examined for metastatic lesions by inspection under a dissection microscope. Indeed, mice injected with

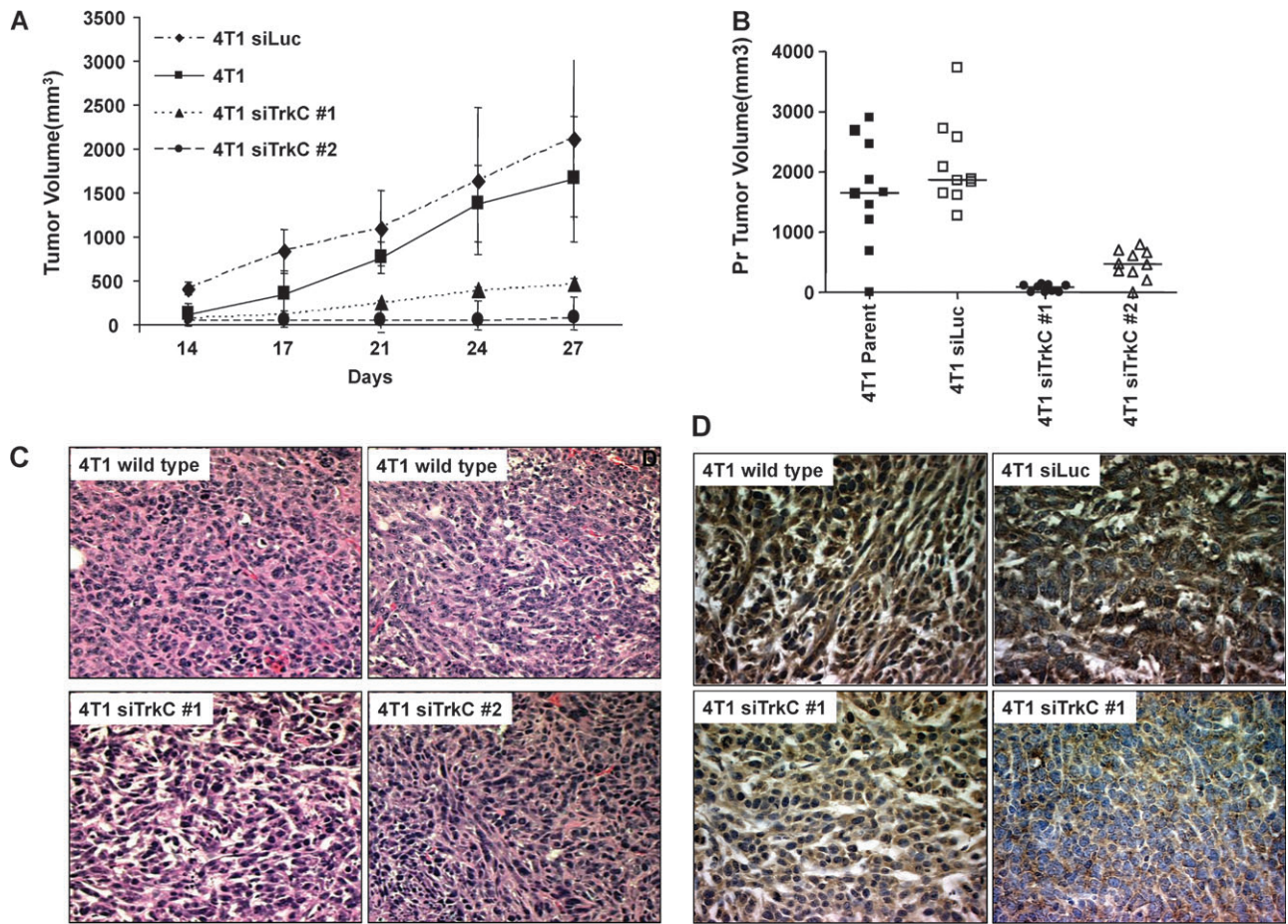


Fig. 4. Suppression of TrkC expression slows primary tumor growth of 4T1 cells in the mammary gland. (A, B) Tumor volumes in primary mammary tumors formed by 4T1 cells expressing either control-siRNA or TrkC-siRNAs. Each data point represents the mean of each type of primary tumor. (C) Hematoxylin and eosin staining of the primary mammary tumors formed by 4T1 cells expressing either control-siRNA or TrkC-siRNAs (magnification: $\times 200$). (D) Immunohistochemical analysis of TrkC protein levels in primary mammary tumors from mice injected with parental 4T1, 4T1 cells expressing control-siRNA or TrkC-siRNAs (magnification: $\times 200$).

trkC-siRNA-transfected cells had significantly fewer metastatic lung nodules than the control counterparts (Figure 5A). Histological analyses confirmed that the number of micrometastatic lesions was also drastically reduced in the lungs of mice carrying *trkC*-siRNA-expressing tumors (Figure 5B and C). Also, phospho-Akt expression was markedly reduced in the lungs of mice carrying *trkC*-siRNA-expressing tumors (Figure 5D).

Taken together, these results clearly show that the knockdown of TrkC reduced lung colonization *in vivo* following implantation of breast cancer cells in the mammary glands. Thus, TrkC seems to be critical in promoting the efficiency of one or more steps in the metastatic process.

Discussion

There is currently great interest in understanding how oncogenic tyrosine kinases function in malignant transformation as these proteins are attractive targets for therapeutic intervention (32). The prevalence of overexpression of the Trk family of neurotrophin receptors in human cancers has also prompted interest in these receptors as potential therapeutic targets (33). In the present study, we showed that TrkC is highly expressed in primary human breast tumors and provided evidence that TrkC is a critical promoter of breast carcinogenesis by demonstrating that TrkC knockdown significantly reduced tumor growth and metastasis of a highly metastatic mammary tumor cell line *in vivo*.

The Trk family of receptors is emerging as an important player in carcinogenic progression. Trks appear to have a high capacity for ligand-independent activation; this has been shown to occur via spontaneous interaction and subsequent autophosphorylation of receptors when Trks are expressed at high levels (34). Many tumors express one or more Trk receptors that may drive aspects of tumor formation and metastasis. Rat intestinal epithelial cells expressing TrkB have been shown to resist anoikis by triggering the activation of the PI3K–Akt cascade (17). TrkA and TrkC can be activated in cancer by chromosomal localization and transcriptional orientation of Trks and its rearranging partners. Somatic rearrangements of TrkA (NTRK1), which produces chimeric oncogenes with constitutive tyrosine kinase activity, have been detected in a consistent fraction of papillary thyroid tumors (35). *ETV6-NTRK3* (*tel-trkC*) fusion transcripts have been identified in congenital fibrosarcoma (a pediatric spindle cell malignancy of the soft tissues), cellular mesoblastic nephroma, acute myeloid leukemia and human secretory breast carcinoma, a rare subtype of infiltrating ductal carcinoma (26,27,36). This fusion gene encodes a unique fusion protein containing the helix-loop-helix protein dimerization domain of Tel and the catalytic domain of TrkC and may contribute to oncogenesis by dysregulation of signal transduction pathways downstream of TrkC. Indeed, expression of *ETV6-NTRK3* causes the transformation of NIH3T3 cells (37), a process that is marked by the induction of cyclin D1 and is dependent on two major effector pathways of wild-type TrkC, the Ras–MAPK pathway and the PI3K–Akt pathway (37).

Supplementary material

Supplementary Figures 1–3 and Table 1 can be found at <http://carcin.oxfordjournals.org/>.

Funding

Korea Healthcare technology R and D Project, Ministry of Health, Welfare and Family Affairs, Republic of Korea (A084024).

Conflict of Interest Statement: None declared.

References

- Bothwell, M. (1995) Functional interactions of neurotrophins and neurotrophin receptors. *Annu. Rev. Neurosci.*, **18**, 223–253.
- Chao, M.V. *et al.* (2002) Neurotrophins: to cleave or not to cleave. *Neuron*, **33**, 9–12.
- Marchetti, D. *et al.* (1993) Nerve growth factor effects on human and mouse melanoma cell invasion and heparanase production. *Int. J. Cancer*, **55**, 692–699.
- McGregor, L.M. *et al.* (1999) Roles of trk family neurotrophin receptors in medullary thyroid carcinoma development and progression. *Proc. Natl Acad. Sci. USA*, **96**, 4540–4545.
- Nakagawara, A. (2001) Trk receptor tyrosine kinases: a bridge between cancer and neural development. *Cancer Lett.*, **169**, 107–114.
- Nicholson, K.M. *et al.* (2003) Autocrine signalling through erbB receptors promotes constitutive activation of protein kinase B/Akt in breast cancer cell lines. *Breast Cancer Res. Treat.*, **81**, 117–128.
- Ricci, A. *et al.* (2001) Neurotrophins and neurotrophin receptors in human lung cancer. *Am. J. Respir. Cell Mol. Biol.*, **25**, 439–446.
- Kogner, P. *et al.* (1993) Coexpression of messenger RNA for TRK proto-oncogene and low affinity nerve growth factor receptor in neuroblastoma with favorable prognosis. *Cancer Res.*, **53**, 2044–2050.
- Nakagawara, A. *et al.* (1994) Expression and function of TRK-B and BDNF in human neuroblastomas. *Mol. Cell. Biol.*, **14**, 759–767.
- Grotzer, M.A. *et al.* (2000) TrkC expression predicts good clinical outcome in primitive neuroectodermal brain tumors. *J. Clin. Oncol.*, **18**, 1027–1035.
- Segal, R.A. *et al.* (1994) Expression of the neurotrophin receptor TrkC is linked to a favorable outcome in medulloblastoma. *Proc. Natl Acad. Sci. USA*, **91**, 12867–12871.
- Yamashiro, D.J. *et al.* (1997) Expression and function of Trk-C in favourable human neuroblastomas. *Eur. J. Cancer*, **33**, 2054–2057.
- Dalal, R. *et al.* (1997) Molecular characterization of neurotrophin expression and the corresponding tropomyosin receptor kinases (trks) in epithelial and stromal cells of the human prostate. *Mol. Cell. Endocrinol.*, **134**, 15–22.
- Weeraratna, A.T. *et al.* (2000) Rational basis for Trk inhibition therapy for prostate cancer. *Prostate*, **45**, 140–148.
- Sakamoto, Y. *et al.* (2001) Expression of Trk tyrosine kinase receptor is a biologic marker for cell proliferation and perineural invasion of human pancreatic ductal adenocarcinoma. *Oncol. Rep.*, **8**, 477–484.
- Douma, S. *et al.* (2004) Suppression of anoikis and induction of metastasis by the neurotrophic receptor TrkB. *Nature*, **430**, 1034–1039.
- Chen-Tsai, C.P. *et al.* (2004) Correlations among neural cell adhesion molecule, nerve growth factor, and its receptors, TrkA, TrkB, TrkC, and p75, in perineural invasion by basal cell and cutaneous squamous cell carcinomas. *Dermatol. Surg.*, **30**, 1009–1016.
- Hisaoka, M. *et al.* (2002) Gene expression of TrkC (NTRK3) in human soft tissue tumours. *J. Pathol.*, **197**, 661–667.
- Satoh, F. *et al.* (2001) Autocrine expression of neurotrophins and their receptors in prostate cancer. *Int. J. Urol.*, **8**, S28–S34.
- Bardelli, A. *et al.* (2003) Mutational analysis of the tyrosine kinome in colorectal cancers. *Science*, **300**, 949.
- Wood, L.D. *et al.* (2006) Somatic mutations of GUCY2F, EPHA3, and NTRK3 in human cancers. *Hum. Mutat.*, **27**, 1060–1.
- Blasco-Gutierrez, M.J. *et al.* (2007) TrkC: a new predictive marker in breast cancer? *Cancer Invest.*, **25**, 405–410.
- Calatozzolo, C. *et al.* (2007) Expression of cannabinoid receptors and neurotrophins in human gliomas. *Neurol. Sci.*, **28**, 304–310.
- Aslakson, C.J. *et al.* (1992) Selective events in the metastatic process defined by analysis of the sequential dissemination of subpopulations of a mouse mammary tumor. *Cancer Res.*, **52**, 1399–1405.
- Miknyoczki, S.J. *et al.* (1999) The Trk tyrosine kinase inhibitor CEP-701 (KT-5555) exhibits significant antitumor efficacy in preclinical xenograft models of human pancreatic ductal adenocarcinoma. *Clin. Cancer Res.*, **5**, 2205–2212.
- Knezevich, S.R. *et al.* (1998) A novel ETV6-NTRK3 gene fusion in congenital fibrosarcoma. *Nat. Genet.*, **18**, 184–187.
- Tognon, C. *et al.* (2002) Expression of the ETV6-NTRK3 gene fusion as a primary event in human secretory breast carcinoma. *Cancer Cell*, **2**, 367–376.
- Song, G. *et al.* (2005) The activation of Akt/PKB signaling pathway and cell survival. *J. Cell. Mol. Med.*, **9**, 59–71.
- Zhao, X. *et al.* (2004) Multiple elements regulate nuclear/cytoplasmic shuttling of FOXO1: characterization of phosphorylation- and 14-3-3-dependent and -independent mechanisms. *Biochem. J.*, **378**, 839–849.
- Gao, D. *et al.* (2009) Phosphorylation by Akt1 promotes cytoplasmic localization of Skp2 and impairs APCcdh1-mediated Skp2 destruction. *Nat. Cell Biol.*, **11**, 397–408.
- Yang, J. *et al.* (2004) Twist, a master regulator of morphogenesis, plays an essential role in tumor metastasis. *Cell*, **117**, 927–939.
- Shawver, L.K. *et al.* (2002) Smart drugs: tyrosine kinase inhibitors in cancer therapy. *Cancer Cell*, **1**, 117–123.
- Ruggeri, B.A. *et al.* (1999) Role of neurotrophin-trk interactions in oncology: the anti-tumor efficacy of potent and selective trk tyrosine kinase inhibitors in pre-clinical tumor models. *Curr. Med. Chem.*, **6**, 845–857.
- Hempstead, B.L. *et al.* (1992) Overexpression of the trk tyrosine kinase rapidly accelerates nerve growth factor-induced differentiation. *Neuron*, **9**, 883–896.
- Pierotti, M.A. *et al.* (2006) Oncogenic rearrangements of the NTRK1/NGF receptor. *Cancer Lett.*, **232**, 90–98.
- Eguchi, M. *et al.* (1999) Fusion of ETV6 to neurotrophin-3 receptor TRKC in acute myeloid leukemia with t(12;15)(p13;q25). *Blood*, **93**, 1355–1363.
- Wai, D.H. *et al.* (2000) The ETV6-NTRK3 gene fusion encodes a chimeric protein tyrosine kinase that transforms NIH3T3 cells. *Oncogene*, **19**, 906–915.
- Brodeur, G.M. *et al.* (1997) Expression of TrkA, TrkB and TrkC in human neuroblastomas. *J. Neurooncol.*, **31**, 49–55.
- Guate, J.L. *et al.* (1999) Expression of p75(LNGFR) and Trk neurotrophin receptors in normal and neoplastic human prostate. *BJU Int.*, **84**, 495–502.
- Rickert, C.H. (2004) Prognosis-related molecular markers in pediatric central nervous system tumors. *J. Neuropathol. Exp. Neurol.*, **63**, 1211–1224.
- Ryden, M. *et al.* (1996) Expression of mRNA for the neurotrophin receptor trkC in neuroblastomas with favourable tumour stage and good prognosis. *Br. J. Cancer*, **74**, 773–779.
- Hoek, K. *et al.* (2004) Expression profiling reveals novel pathways in the transformation of melanocytes to melanomas. *Cancer Res.*, **64**, 5270–5282.
- Maestro, R. *et al.* (1999) Twist is a potential oncogene that inhibits apoptosis. *Genes Dev.*, **13**, 2207–2217.
- Rosivatz, E. *et al.* (2002) Differential expression of the epithelial-mesenchymal transition regulators snail, SIP1, and twist in gastric cancer. *Am. J. Pathol.*, **161**, 1881–1891.
- van Doorn, R. *et al.* (2004) Aberrant expression of the tyrosine kinase receptor EphA4 and the transcription factor twist in Sezary syndrome identified by gene expression analysis. *Cancer Res.*, **64**, 5578–5586.
- Barnabe-Heider, F. *et al.* (2003) Endogenously produced neurotrophins regulate survival and differentiation of cortical progenitors via distinct signaling pathways. *J. Neurosci.*, **23**, 5149–5160.

Received April 29, 2010; revised August 10, 2010; accepted August 21, 2010